Journal of the Korean Ceramic Society
Vol. 43, No. 8, pp. 451~457, 2006.

Review

Materials Development in α-Sialon Ceramics

Mamoru Mitomo,† Rong-Jun Xie, and Naoto Hirosaki

National Institute for Materials Science, Namiki, Tsukuba, Ibaraki 305-0044, Japan
(Received May 23, 2006; Accepted May 24, 2006)

ABSTRACT

The solid solutions of α-Si_3N_4, i.e. α-sialons, are represented by a general formula of $M_x(Si,Al)_{12}(O,N)_{16}$, in which metal ions (M) dissolve into interstitial sites to stabilize the structure. Processing methods for the fabrication of α/β-sialon composites, α-sialon/β-Si_3N_4 composites, refractory or tough α-sialon ceramics have been developed to tailor the mechanical properties. Translucent and photoluminescent properties have been investigated recently. A number of applications of α-sialon ceramics as engineering and optical ceramics are also presented.

Key words*: *α-sialon, Microstructure, Engineering ceramics, Photoluminescence, White LED

1. Introduction

The sintering of silicon nitride (Si_3N_4) has been investigated to optimize the mechanical properties and for applications in engineering ceramics.[1] Densification results from a liquid phase sintering with oxide additives.[2] High α powders have been used to fabricate strong and tough ceramics. The additives form a liquid phase at the sintering temperature through a reaction with Si_3N_4 and the surface silica of the powder. The densification is accompanied by the solution of α-grains, diffusion through the liquid, and precipitation as β-grains. The microstructure development is largely related to this phase transformation from α (trigonal, space group: P31c) to β (hexagonal, space group: $P6_3/m$). The Si-N bond is mainly based on covalent bonding. Most additives do not dissolve into Si_3N_4 and remain as glassy or crystalline phases at the grain boundaries after sintering.

Some additives, for example Al_2O_3, react with Si_3N_4 to form a solid solution. The solid-liquid phase relation in this system is shown in Fig. 1.[3] The solid solution is represented by a general formula, $Si_{6-z}Al_zO_zN_{8-z}$ (βss in the figure), as the number of atoms corresponding to the two formulas are included in a unit cell. The materials has been referred to as β-sialon from its chemical composition (Si-Al-O-N) and crystal structure. The formula indicates that the Si-N bond in β-silicon nitride is replaced by Al-O and Al-N bonds so as to maintain the metal/nonmetal ratio at 3/4. The starting materials for the sintered β-sialon is the mixture in the system Si_3N_4-Al_2O_3-AlN or Si_3N_4-SiO_2-AlN. The starting mixture reacts at high temperatures and forms a liquid phase (L in the figure). The starting powders dissolve in the liquid and precipitate as β-sialon grains. Therefore, the amount of the liquid phase decreases and the chemical composition changes upon sintering. Such sintering behavior is termed "transient liquid phase sintering". Most liquid phases dissolve into the grains after sintering. When the total chemical composition of the starting mixture is strictly controlled, the grain boundary glassy phase completely disappears, resulting in single phase α-sialon ceramics.

Consequently, the solid solution of α-Si_3N_4, i.e., α-sialon, was found.[4,5] The sintering and the measurements of the mechanical properties of this have also been attemped.[6] In the present review, the characteristics of the crystal structure, the mechanical properties and the optical properties of α-sialon ceramics are summarized. Some applications as engineering ceramics and optical ceramics are also presented.

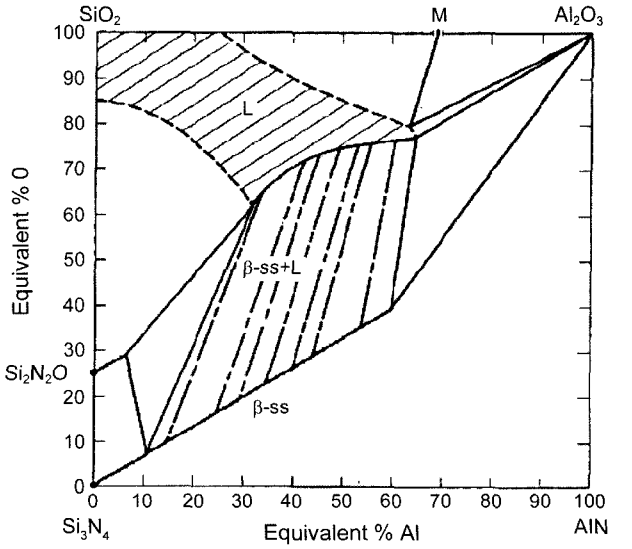

Fig. 1. Phase relationship in the Si_3N_4-SiO_2-AlN-Al_2O_3 system.

†Corresponding author : Mamoru Mitomo
E-mail : mitomo.mamoru@nims.go.jp
Tel : +81-298-51-3354 Fax : +81-298-52-7449

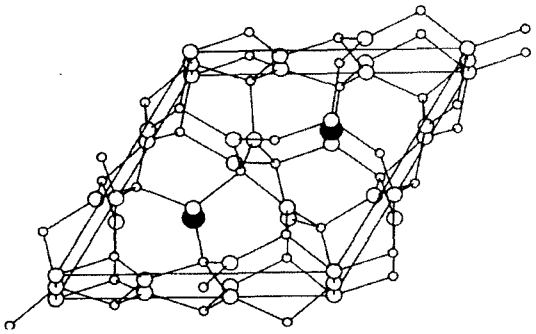

Fig. 2. Structure model for α-sialon (large black sphere represents interstitial sites).

2. Characteristics of α-Sialons

The crystal structure of α-sialon in hexagonal system is shown in Fig. 2. There are two large interstitial sites in a unit cell. The general formula for the solid solution is $M_x(Si,Al)_{12}(O,N)_{16}$, in which M=Li, Mg, Ca, Y or lanthanide metals, except for La and Ce. This is based on the fact that four formulas are included in a unit cell. The interstitial dissolution of metals (M) stabilizes α-Si_3N_4 structure, otherwise it transforms to β at a high temperature. To maintain the neutrality, a number of the Si-N bonds in the framework structure are replaced by Al-N and Al-O bonds. The electronegativity and ionic radius of the dissolving ions is in the range of 1.0 - 1.3 and <0.1 nm, respectively. The interstitial ion is surrounded by seven O+N atoms. It is interesting to note that the chemical bonding in the framework is based mainly on covalent bonding, whereas the metals are dissolved as ions.

The unit cell dimension and relative intensity in the powder X-Ray Diffraction profile (XRD) changes as a result of the dissolution of the metal ions. The structure was confirmed by a Rietveld analysis, which compared the observed XRD with the calculated XRD using Ca-α-sialon as an example (Fig. 3).[7] The ionic radius of La (0.115 nm), like that of Ce(0.111 nm) was too large to simply occupy the interstitial sites. When they were co-doped with a typical

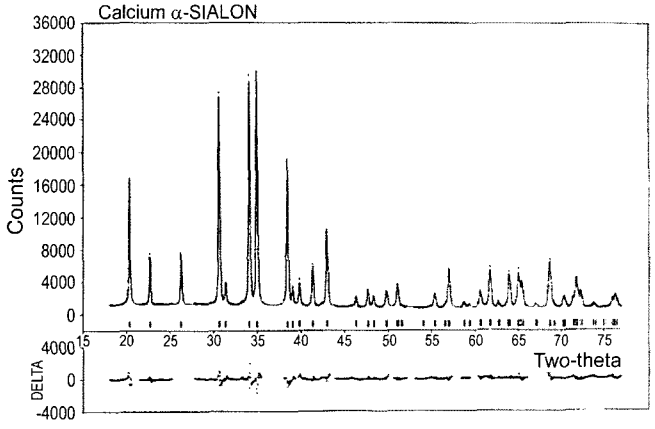

Fig. 3. Rietveld analysis of Ca-α-sialon.

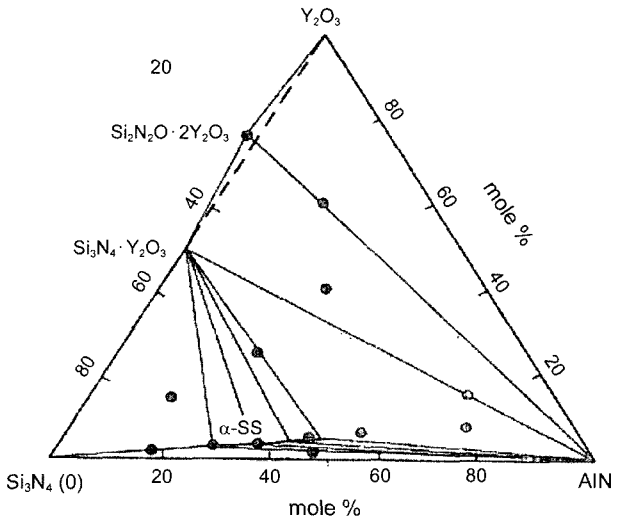

Fig. 4. The range of α-sialon formation (α-ss) in the Si_3N_4-AlN-Y_2O_3 system.

stabilizing metal such as Ca or Y,[8,9] or if they were fabricated under special conditions,[10] only a small fraction dissolved into the grains, leading to planar defects.[9,11] These results show that small ions dissolve into interstitial sites randomly without structure strain, whereas large ions cause a large strain and result in defects.

The range of α-sialon formation (α-ss) in an Si_3N_4-Y_2O_3-AlN system at 1700°C is shown in Fig. 4.[12] Both a maximum and a minimum for the α-sialon formation are shown. There should be a miscibility gap between α-sialon and β-Si_3N_4, as β-Si_3N_4 is stable in a pure system at high temperatures, and continuous solid solubility should therefore be impossible.

A more general formula for α-sialon is, $M_{m/v}Si_{12-(m+n)}Al_{(m+n)}O_nN_{16-n}$, in which v is the valence of the dissolving ion, m is the number of Al-N bonds, and n the number of A-O bonds in a unit cell. The m value is directly related to the amount of ions, as shown in the general formula. As suggested from Fig. 4, α-sialon is a very nitrogen rich solid solution compared to β-sialon. The solid solution range depends on the ionic size of the stabilizing ion, as in Fig. 5.[13] The maximum solubility increases with the decrease of the ionic size. This may be due to the rigid and covalent framework structure. The lower limit is always a constant of m=1, implying that the solid solubility of the metal (x) is 0.33 for trivalent ions. The critical amount is very small: one ion in three-unit cells with six available interstitial positions. The reason for this critical value is not understood as yet.

It has been reported that the unit cell size of hexagonal α-sialon depends only on the m and n values, and is independent of the type and size of the ion.[14]

$$a\ (nm) = (7.752 + 0.036m + 0.02n) \times 10^{-1}$$
$$c\ (nm) = (5.620 + 0.031m + 0.04n) \times 10^{-1}$$

It has also been reported that the solubility depends also on the temperature, and increases at higher tempera-

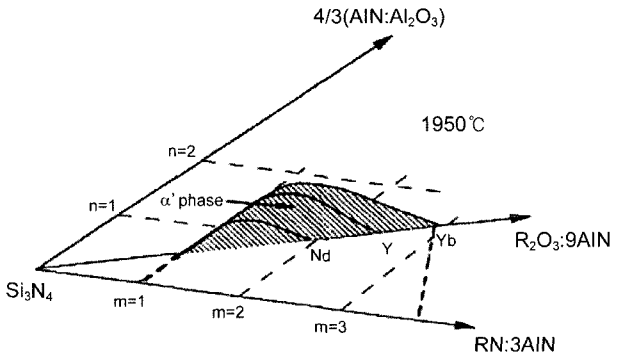

Fig. 5. The change in the solubility range of α-sialon with the type of ion at 1950°C.

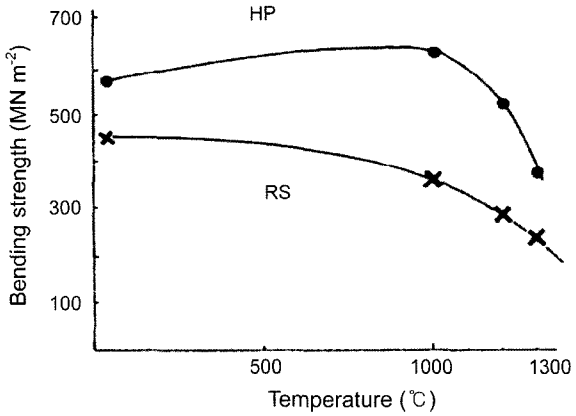

Fig. 6. The change of three point bending strength of hot-pressed (HP) and the reaction sintered (RS) α-sialon ceramics with temperature.

tures.[13,15] Therefore, the α/β ratio and resultant microstructure in α-sialon ceramics are largely dependent on the type and the amount of ion, as well as processing conditions.

A preliminary investigation regarding the bending strength of the Y-α-sialon was conducted with hot-pressed and reaction sintered materials.[6] The change in the bending strength according to the temperature is indicated in Fig. 6. The values are nearly equivalent to those of sintered silicon nitride. The thermal expansion coefficients and thermal conductivities of the α-sialons[16,17] are in the range of $3.8\text{-}4.0\times10^{-6}$/°C and are 18-20 W/mK, respectively. The former is higher and the latter is lower than those values of silicon nitride ceramics. This is likely due to the interstitial dissolution of the ions. The results represent the possibility of α-sialons as engineering ceramics at high temperatures.

3. Materials Development as Engineering Ceramics

3.1. α/β-Sialon Composites

α-sialons are less sinterable as compared to β-sialons due to the smaller amount of transient liquid. It has been shown that the addition of sintering additives, which do not dissolve in α-sialon grains, was effective for densification.[14] It is known that the α content in the α/β-sialon is related to the metallic composition and nitrogen content in the starting compacts, in addition to the type of metals.[18] A high nitrogen content in the composition and a smaller ionic radius of the stabilizing ion both serve to increase the α-sialon content. This demonstrates that the partition function of added metal in grains and at grain boundaries increases in small ions. To optimize the mechanical properties and thermal stability, the addition of dual lanthanides with different solubilities and sinterabilities was attempted.[19] The α/β-sialon composites were also fabricated from the compact in the system Si_3N_4-M_2O_3-Al_2O_3-AlN in accordance with the phase relationships. Thus, the α/β ratio and resultant microstructure were controlled not only by the thermodynamic but also by the kinetic parameters. The hardness of α-sialons is higher than that of silicon nitride ceramics. For this reason, the α-sialon material has been applied as cutting tools for Inconel superalloys.[20]

3.2. α-Sialon/β-Si_3N_4 Composites-Partially Stabilized α-Sialons

As suggested from the phase relations in Fig. 4, the addition of a minimum amount of stabilizing metal is necessary to fabricate single phase α-sialon ceramics. The starting mixture for the Y-α-sialon is

$$Si_3N_4 + 1/2x(Y_2O_3 + 9AlN)$$

When the amount of additives is less than the critical level of x=0.3, the sintered materials are composed of α-sialon and β-Si_3N_4. These materials are known as "partially stabilized α-sialons", which are composed of spherical α-sialon grains and elongated β-Si_3N_4 grains. A TEM micrograph of a partially stabilized α-sialon is compared to that of a "fully" stabilized α-sialon in Fig. 7.[21,22] The bending strength increases with an increase in the β-Si_3N_4 content, whereas the hardness has the opposite tendency, as shown in Fig. 8. The strength values were further improved by HIP treatment at 1800°C under 200 MPa N_2 after pressureless sinter-

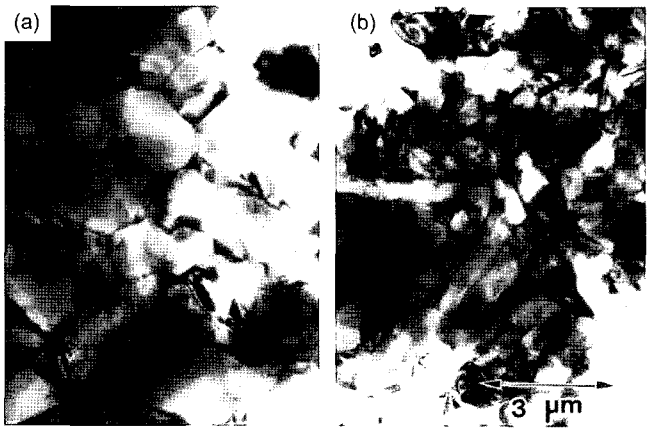

Fig. 7. TEM micrographs of (a) "fully stabilized α-sialon" and (b) "partially stabilized α-sialon" with spherical α-sialon grains and elongated β-Si_3N_4 grains.

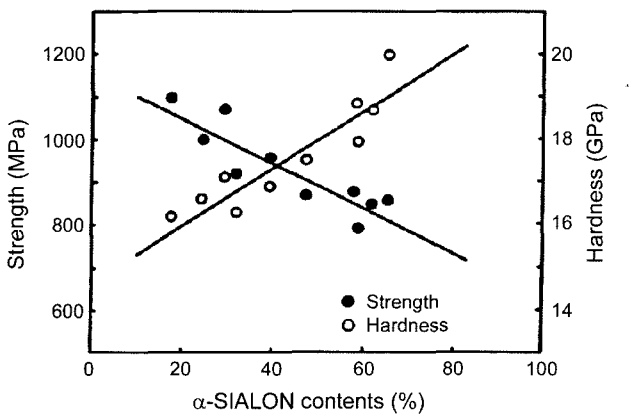

Fig. 8. The change of hardness and bending strength with the α content in partially stabilized α-sialon ceramics.

Table 1. Bending Strength of Sintered and the HIPped α-Sialon Ceramics

	A	B (x=0.15)	C (x=0.2)
Sintering method	Pressureless	HIP	HIP
Density (g/cm^3)	3.22	3.23	3.24
α-Sialon contents (%)	30	20	45
Hardness, Hv (GPa)	16.2	16.5	18.0
Bending strength (MPa)			
R.T.	980	1350	1400
1200°C	600	950	900

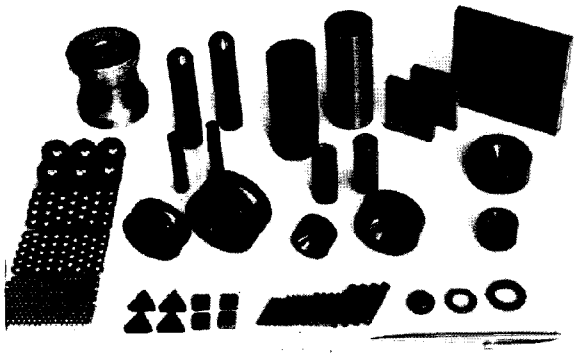

Fig. 9. Ceramic components applied in industry (Courtesy Shinagawa Refractory Co.).

ing.[23] The mechanical properties of partially stabilized α-sialons after HIP treatment are listed and compared to those of the sintered materials in Table 1. The materials have good corrosion and erosion resistance at intermediate temperatures of 500-1000°C. A number of components that have been developed are shown in Fig. 9. Among these applications are guide rollers for extruding non-ferrous metals, bonding capillaries for wiring Au in LSI, milling balls, and nozzles for metal welding.

3.3. Refractory α-Sialon Ceramics

A large amount of grain boundary phase is beneficial for densification, whereas the strength deteriorates at high temperatures, as in silicon nitride ceramics. One way to solve this problem is to find an additive which produces a large amount of transient liquid phase and then consolidates as refractory grain boundary phases. YAG (Yttrium Aluminum Garnet) was determined to be a compatible grain boundary phase with a high melting temperature.[24,25] The additives formed a liquid phase at the sintering temperature and accelerated the sintering. The liquid solidified as a glassy phase after cooling. A high-resolution TEM (HRTEM) micrograph revealed that the wetting angle was very low and that all grains were completely covered by the liquid phase. A thin amorphous film remained between the α-sialon grains, as shown in Fig. 10(a).[2,5] The annealing of the materials at 1450°C resulted in the crystallization of YAG at multiple grain junctions. It is interesting that the grain boundary phase was completely withdrawn from the boundaries, and that direct bonding between α-sialon grains was attained (Fig. 10(b)). High temperature bending strength could be improved, as shown in Fig. 11.[26] These results indicate that high temperature strength largely depends not only on crystallization but also on the nano-

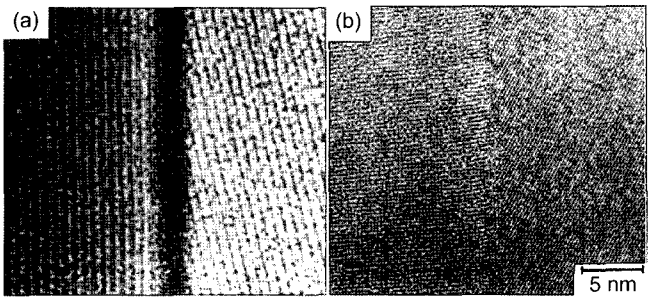

Fig. 10. HRTEM micrographs of the grain boundary in (a) the as-sintered materials and (b) the sintered and annealed material.

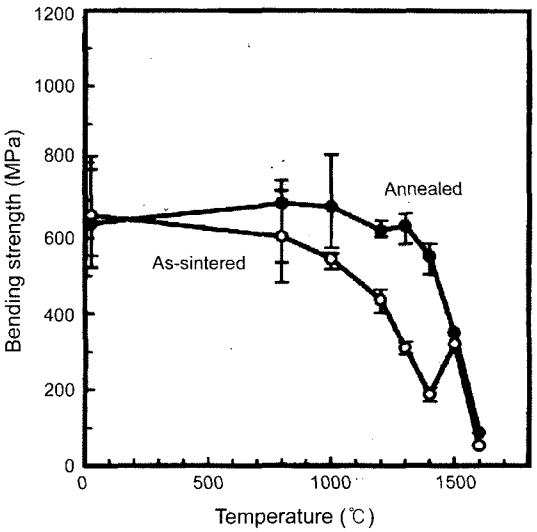

Fig. 11. The change of bending strength of as-sintered and annealed materials with temperature.

structure at the grain boundaries. The importance of the nano-structure at the grain boundaries was also reported for SiC ceramics.[27,28] It is likely that a wetting/dewetting transition occurred in the grain boundaries together with a vitrification/devitrification transition at approximately 1400°C. It is necessary to find an additive, that is compatible with α-sialon and has a higher transition temperature in order to further improve the high temperature strength.

3.4. Tough α-Sialon Ceramics

When fully stabilized α-sialon ceramics were fabricated by pressureless sintering, the materials were composed of spherical grains, as shown in Fig. 7(a). With this type of microstructure, the fracture toughness values were fairly low in the absence of any toughening mechanism. To increase the fracture toughness, abnormal grain growth of a small number of grains in a fine-grained matrix has attempted in fully stabilized α-sialon ceramics. This represents an identical approach as "in-situ reinforcement" in silicon nitride[29] and silicon carbide ceramics.[30] One way to develop in-situ reinforced microstructures is to use a phase transformation from β-Si_3N_4 to α-sialon during sintering.[31] The relationship between the fracture toughness of ceramics, the amount of elongated grains and the ionic radius of the stabilizing metal indicates that a larger ion leads to a greater amount of abnormal grains and a high fracture toughness, although the values remained inadequate for 5-5.5 $MPam^{1/2}$. Another method is to apply a post-sintering heat-treatment at 1900°C.[32] A number of grains grew abnormally during annealing. Although fairly good in-situ reinforced microstructures were developed, the fracture toughness values were lower than expected. The reason for this may be related to the large fraction of intragranular fracture. The results here indicate that not only the microstructure control but also an understanding of the microfracture mechanics is important for further toughening.

4. Materials Development as Optical Ceramics

4.1. Translucent α-Sialon Ceramics

The color of sintered α-sialon ceramics is usually gray or black. However, translucent α-sialon ceramics can be fabricated by choosing the stabilizing ion and optimizing sintering conditions that increase the grain size and decrease the amount of grain boundary phase.[33] It has been reported that a fairly high transmittance of nearly 70% in the visible light region was attained in 0.5 mm thick Lu-stabilized α-sialon ceramics.[34]

4.2. Photoluminescent Properties

Photoluminescence is based on a transition of the electronic state from an activated state to a ground state. The emission wavelength depends not only on the energy gap but also on the crystal field surrounding the ions. It has been shown that the doping of rare-earth metals in Y-Si-O-N compounds[35] or $LaSi_3N_5$[36] leads to longer wavelength

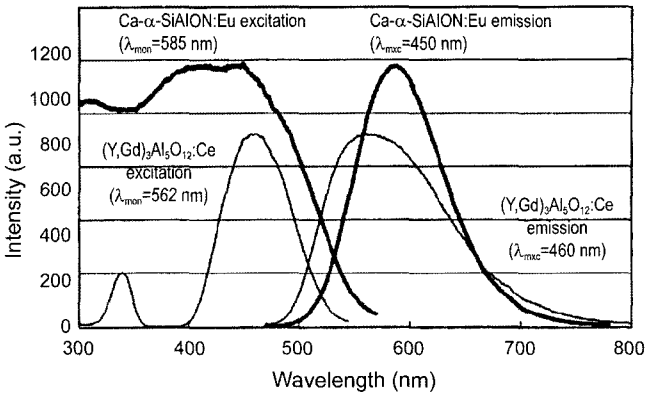

Fig. 12. Excitation and emission spectra of Ca-α-sialon:Eu and YAG:Ce.

emissions compared to corresponding oxides, i.e., the red shift. The excitation and emission spectra of α-sialons[37,38] were measured. It is well known that most photoluminescent materials can be excited under a high energy such as UV light. However, a number of the α-sialons can be excited with visible light. It was suspected that α-sialons may be good host lattice for phosphors due to the following factors: (1) their high nitrogen content, (2) flexibility in tailoring the excitation and emission spectra,[39] (3) high temperature stability, (4) their reactive, stable and available starting powders. The excitation and emission spectra of Eu^{2+}-doped Ca-α-sialon are compared with those of Gd, Ce-doped YAG (YAG:Ce) phosphor in Fig. 12.[39] This figure indicates that the α-sialon phosphor can be excited by InGaN based blue LED with a wavelength of approximately 450-460 nm. The excitation and emission spectra can be tailored by doping different ion, i.e. Ce^{3+},[41] Yb^{2+},[42] or Li^+.[43] The maximization of the emission intensity or the tuning of the excitation and emission wave length are the subject of future studies that can lead to further improvements in this area.

4.3. Application as Phosphors for White LEDs

Recently, a white LED was invented using a blue LED as an excitation beam and YAG:Ce phosphor as a wavelength convertor.[44] A cut model of a type of white LED is shown in Fig. 13[45] and a photograph of the LED unit is shown in Fig. 14. The phosphor is mounted on the top of blue LED that converts the light into yellow or orange. The mixed light shows quasi-white. White LED components are now widely used in various types of illuminations and as a backlight for cellular phones. The benefits of white LED are its high efficiency, long lifetime and high reliability. If the emission efficiency is further improved, widely used fluorescent lamps may eventually be replaced by white LEDs. The use of toxic Hg can be avoided in the lightening industry. Fig. 15 shows the change in the normalized emission intensity on the temperature in comparison with that of YAG:Ce. The drop in intensity is very small for the α-sialon phosphor, while it decreases sharply in the case of YAG:Ce. It is clear α-sialons have advantages for applications under severe conditions.

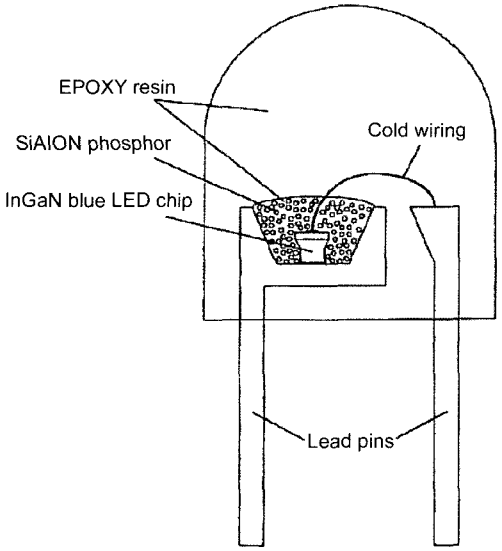

Fig. 13. Cut model of a white LED with α-sialon phosphor.

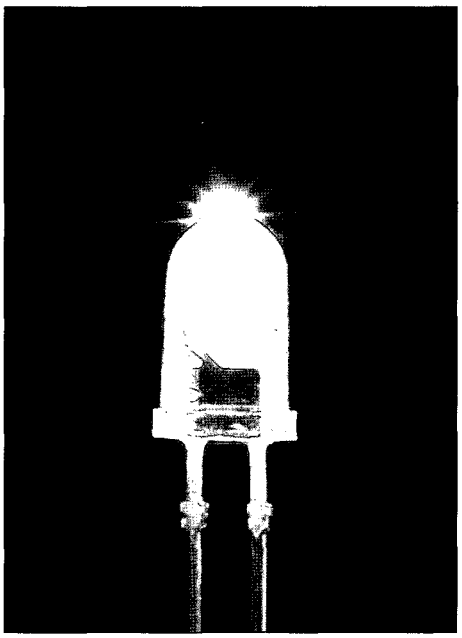

Fig. 14. Photograph of a white LED unit (Courtesy K. Sakuma, Fujikura Ltd.).

5. Summary

The micro- and nano-structure of α-sialon ceramics was controlled by the type and amount of additives as well as by the processing conditions. Composite ceramics, refractory or tough α-sialon ceramics were developed in order to optimize the mechanical properties of engineering ceramics in a medium temperature range. Optical ceramics, i.e. translucent and photoluminescent α-sialon ceramics, were developed recently; the materials development for the proposed α-sialon ceramics is closely related to this special crystal structure, with a covalent framework and interstitial ions.

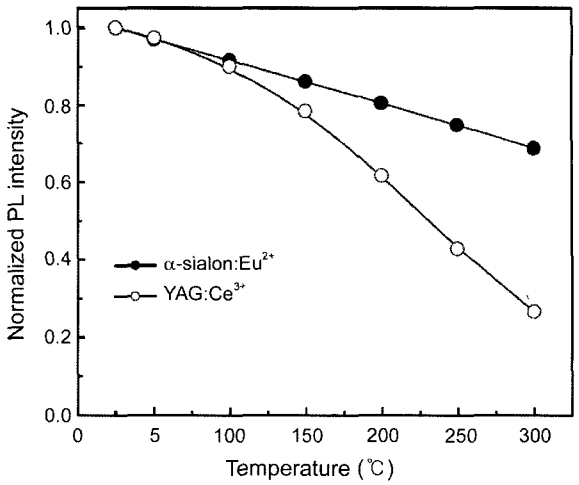

Fig. 15. Temperature dependence of normalized emission intensity in Ca-α-sialon:Eu and YAG:Ce.

REFERENCES

1. M. Mitomo and Y. Tajima, "Sintering, Properties and Applications of Silicon Nitride and Sialon Ceramics," *J. Ceram. Soc. Jpn.*, **99** 1014-25 (1991).
2. M. Mitomo. "Pressure Sintering of Si_3N_4," *J. Mater. Sci.*, **11** 1103-07 (1976).
3. I. K. Naik, L. J. Gauckler, and T. Y. Tien, "Solid-Liquid Equilibria in the System Si_3N_4-AlN-SiO_2-Al_2O_3," *J. Am. Ceram. Soc.*, **61** 332-35 (1978).
4. G. Grand, J. Demit, J. Ruste, and J. P. Torre, "Composition and Stability of Y-Si-Al-O-N Solid Solution Based on α-Si_3N_4 Structure," *J. Mater. Sci.*, **14** 1749-51 (1979).
5. S. Hampshire, H. K. Park, D. P. Thompson, and K. H. Jack, "α'-Sialon Ceramics," *Nature*, **274** 880-82 (1978).
6. M. Mitomo, H. Tanaka, K. Muramatsu, N. Ii, and Y. Fujii, "The Strength of α-Sialon Ceramics," *J. Mater. Sci.*, **15** 2661-62 (1980).
7. F. Izumi, M. Mitomo, and Y. Bando, "Rietveld Refinements for Calcium and Yttrium Containing α-Sialons," *J. Mater. Sci.*, **19** 3115-20 (1984).
8. H. Mandal and M. J. Hoffmann, "Preparation of Multiple-cation α-SiAlON Ceramics Containing Lanthanum," *J. Am. Ceram. Soc.*, **82** 229-32 (1999).
9. T. Ekstroem, K. Jansson, P. O. Olsson, and J. Persson, "Formation of an Y/Ce-Doped α-Sialon Phase," *J. Eur. Ceram. Soc.*, **8** 3-9 (1991).
10. C. M. Wang, M. Mitomo, F. F. Xu, N. Hirosaki, and Y. Bando, "Synthesis of Cerium-α-SiAlON with Nuclei Addition," *J. Am. Ceram. Soc.*, **84** 1389-91 (2001).
11. F. F. Xu, Y. Bando, C. M. Wang, and M. Mitomo, "Domain-Boundary Structures in Ce-Doped α-(Si-Al-O-N)," *Phil. Mag.*, **81** 2771-84 (2001).
12. Z. K. Huang, P. Greil, and G. Petzow, "Formation of α-Si_3N_4 Solid Solutions in the System Si_3N_4-AlN-Y_2O_3," *J. Am. Ceram. Soc.*, **66** C-96-7 (1983).
13. A. Rosenflanz and I. W. Chen, "Kinetics of Phase Transformations in SiAlON Ceramics: I. Effects of Cation Size, Composition, and Temperature," *J. Eur. Ceram. Soc.*, **19**

2325-35 (1999).
14. Z. Shen and M. Nygren, "On the Extension of the α-Sialon Phase Area in Yttrium and Rare-Earth Doped Systems," *J. Eur. Ceram. Soc.*, **17** 1639-45 (1997).
15. M. Mitomo and A. Ishida, "Stability of α-Sialons in Low Temperature Annealing," *J. Eur. Ceram. Soc.*, **19** 7-15 (1999).
16. M. Mitomo, F. Izumi, P. Greil, and G. Petzow, "Thermal Expansion of α-Sialon Ceramics," *Am. Ceram. Soc. Bull.*, **63** 730 (1984).
17. M. Mitomo, N. Hirosaki, and T. Mitsuhashi, "Thermal Conductivity of α-Sialon Ceramics," *J. Mater. Sci. Lett.*, **3** 915-16 (1984).
18. N. Camscu, D. P. Thompson, and H. Mandal, "Effect of Starting Composition, Type of Rare Earth Sintering Additive and Amount of Liquid Phase on α-β Sialon Transformation," *J. Eur. Ceram. Soc.*, **17** 599-613 (1997).
19. C. Zhang, W. Y. Sun, and D. S. Yen, "Optimizing Mechanical Properties and Thermal Stability of Ln-α-β-Sialon by Using Duplex Ln Elements (Dy and Sm)," *J. Eur. Ceram. Soc.*, **19** 33-9 (1999).
20. H. Mandal, F. Kara, S. Turan, and A. Kara, pp. 193-202 in SiAlONs. Ed. by K. Komeya, M. Mitomo, and Y. B. Cheng, Trans Tech. Publications, Switzerland, 2003.
21. K. Ishizawa, N. Ayuzawa, A. Shiranita, M. Takai, N. Uchida, and M. Mitomo, "Properties of α-Sialon Ceramics," *J. Ceram. Soc. Jpn.*, **94** 193-96 (1986).
22. K. Ishizawa, N. Ayuzawa, H. Haishi, A. Shiranita, M. Takai, and M. Mitomo, "Some Properties and Applications of α-Sialon Ceramics," pp. 239-50 in Silicon Nitride 2. Ed. by M. Mitomo and S. Somiya, Uchida-Rohkakuho, Tokyo, 1990 (in Jpn.).
23. A. Shiranita, K. Ishizawa, N. Ayuzawa, M. Takai, M. Yoshizawa, and M. Mitomo, "Microstructural Characterization of Yb-α-Sialon Ceramics Prepared by Post Sintering HIP Treatments," pp. 907-20 in Advanced Materials '93, IA : Ceramics, Powders, Corrosion and Advanced Processing, Elsevier Science, Amsterdam, 1994.
24. J. H. Min and M. Mitomo, "Preparation of Y-α-Sialon with Glassy or Crystalline Phases at Grain Boundaries," *Ceram. Int.*, **21** 487-92 (1995).
25. M. Mitomo, T. Nishimura, and Y. Kitami, "High Temperature Properties and Grain Boundary Structure in Silicon Nitride Based Ceramics," pp. 275-80 in Ceramic Transaction 118, *Am. Ceram. Soc.* (2000).
26. T. Nishimura, M. Mitomo, A. Ishida, and H. Gu, "Improvement of High Temperature Strength and Creep of α-Sialon by Grain Boudary Crystallization," *Key Eng. Mater.*, **171-174** 741-44 (2000).
27. H. J. Choi, Y.-W. Kim, M. Mitomo, T. Nishimura, J. H. Lee, and D. Y. Kim, "Intergranular Glassy Phase Free SiC Ceramics Retain Strength at 1500°C," *Scripta Mater.*, **50** 1203-07 (2004).
28. Y.-W. Kim, S. H. Lee, T. Nishimura, and M. Mitomo, "Heat-Resistant Silicon Carbide with Aluminum Nitride and Scandium Oxide," *Acta Mater.*, **53** 4701-08 (2005).
29. M. Mitomo and S. Uenosono, "Microstructural Development During Gas-Pressure Sintering of α-Silicon Nitride," *J. Am. Ceram. Soc.*, **75** 103-08 (1992).
30. S. G. Lee, Y.-W. Kim, and M. Mitomo, "Relation between Microstructure and Fracture Toughness of Toughened Silicon Carbide Ceramics," *J. Am. Ceram. Soc.*, **84** 1347-53 (2001).
31. I. W. Chen and A. Rosenflanz, "A Tough SiAlON Ceramic Based on α-Si_3N_4 with a Whisker-Like Microstructure," *Nature*, **389** 701-04 (1997).
32. C. Zhang, K. Komeya, J. Tatami, and T. Meguro, "Inhomogeneous Grain Growth and Elongation of Dy-α-Sialon Ceramics at Temperatures above 1800°C," *J. Eur. Ceram. Soc.*, **20** 939-44 (2000).
33. H. Mandal, "New Developments in α-SiAlON Ceramics," *J. Eur. Ceram. Soc.*, **19** 2349-57 (1999).
34. M. J. Jones, H. Hyuga, K. Hirao, and Y. Yamauchi, "Highly Transparent Lu-α-SiAlON," *J. Am. Ceram. Soc.*, **87** 714-16 (2004).
35. J. W. H. Krevel, H. T. Hintzen, R. Metselaar, and A. Meijerink, "Long Wavelength Ce^{3+} Emmision in Y-Si-O-N Materials," *J. Alloy Comp.*, **268** 272-77 (1998).
36. K. Uheda, R. Takizawa, T. Endo, H. Yamane, M. Shimada, C. M. Wang, and M. Mitomo, "Synthesis and Luminescent Properties of Eu-Doped $LaSi_3N_5$ Phosphor," *J. Lumin.*, **81-89** 967-69 (2000).
37. R. J. Xie, M. Mitomo, K. Uheda, F. F. Xu, and Y. Akimune, "Preparation and Luminescence Spectra of Calcium- and Rare-Earth (R=Eu, Tb, and Pr)-Doped α-SiAlON Ceramics," *J. Am. Ceram. Soc.*, **85** 1229-34 (2002).
38. J. W. H. Krevel, J. W. T. Rutten, H. Mandal, H. T. Hintzen, and R. Metselaar, "Luminescence Properties of Terbium-, Cerium, or Europium-Doped α-Sialon Materials," *J. Solid State Chem.*, **165** 19-24 (2002).
39. R. J. Xie, N. Hirosaki, M. Mitomo, T. Suehiro, X. Xu, and H. Tanaka, "Photo-Lluminescence of Rare-Earth-Doped Ca-α-SiAlON Phosphors : Composition and Concentration Dependence," *J. Am. Ceram. Soc.*, **88** 2883-88 (2005).
40. K. Sakuma, K. Omichi, N. Kimura, M. Ohashi, D. Tanaka, N. Hirosaki, Y. Yamamoto, R. J. Xie, and T. Suehiro, "Warm-White Light-Emitting Diode with Yellowish Orange SiAlON Ceramic Phosphor," *Opt. Lett.*, **29** 2001-03 (2004).
41. R. J. Xie, N. Hirosaki, M. Mitomo, Y. Yamamoto, T. Suehiro, and N. Ohashi, "Photo-Luminescence of Cerium-Doped α-SiAlON Materials," *J. Am. Ceram. Soc.*, **87** 1368-70 (2004).
42. R. J. Xie, N. Hirosaki, M. Mitomo, K. Uheda, T. Suehirc, X. Xu, Y. Yamamoto, and T. Sekiguchi, "Strong Green Emission from α-SiAlON Activated by Divalent Ytterbium under Blue Light Irradiation," *J. Phys. Chem.*, **B109** 9490-94 (2005).
43. R. J. Xie, N. Hirosaki, M. Mitomo, K. Takahashi, and K. Sakuma, "Highly Efficient White-Light Emitting Diodes Fabricated with Short-Wavelength Yellow Oxynitride Phosphors," *Appl. Phys. Lett.*, **88** 101104/1-3 (2006).
44. T. Mukai and S. Nakamura, "White and UV LEDs," *Ohbutsu(Appl. Phys.)*, **68** 152-55 (1998) (in Jpn.).
45. K. Sakuma, N. Hirosaki, N. Kimura, M. Ohashi, R. J. Xie, Y. Yamamoto, T. Suehiro, K. Asano, and D. Tanaka, "White Light-Emitting Diode Lamps Using Oxynitride and Nitride Phosphor Materials," *IEICE Elect.*, **E88-C** 2057-64 (2005).